European Journal of Pharmaceutics and Biopharmaceutics 141 (2019) 100–110

Contents lists available at ScienceDirect

European Journal of Pharmaceutics and Biopharmaceutics

journal homepage: www.elsevier.com/locate/ejpb

Research paper

Post-manufacture loading of filaments and 3D printed PLA scaffolds with prednisolone and dexamethasone for tissue regeneration applications

Xián Farto-Vaamonde[a,1], Giulia Auriemma[b,1], Rita Patrizia Aquino[b], Angel Concheiro[a], Carmen Alvarez-Lorenzo[a,*]

[a] Departamento de Farmacología, Farmacia y Tecnología Farmacéutica, R + DPharma Group (GI-1645), Facultad de Farmacia and Health Research Institute of Santiago de Compostela (IDIS), Universidade de Santiago de Compostela, 15782 Santiago de Compostela, Spain
[b] Department of Pharmacy, University of Salerno, Via Giovanni Paolo II 132, I-84084 Fisciano (SA), Italy

ARTICLE INFO

Keywords:
Fused deposition modeling
3D printing
Controlled release
Poly(L-lactic acid)
Prednisolone
Dexamethasone
Regenerative medicine
Post-manufacture loading

ABSTRACT

Strategies to load prednisolone or dexamethasone in preformed poly(L-lactic acid) (PLA) filaments and 3D printed scaffolds were explored as a way of personalizing the drug, the dose and the release profile for regenerative medicine purposes. Instead of starting from a PLA filament preloaded with a given content of drug, we explored two more versatile strategies. The first one involved the soaking of PLA filaments into a drug solution prepared in a solvent that reversibly swelled PLA; during 3D printing the melting of PLA contributed to the efficient integration (encapsulation) of the drug inside the printed strand. The second strategy consisted in first printing the 3D PLA scaffolds followed by soaking in a suitable drug solution in order to exploit the higher specific surface of the printed strands compared to the filament. Sustained release profiles were recorded when either prednisolone or dexamethasone were loaded in preformed PLA filaments, while rapid release was recorded for 3D PLA scaffolds loaded after printing. The combination of the two proposed methods reported here opened the possibility of creating concentration gradients of different drugs in the same scaffold exhibiting distinct release patterns. Namely, the strand core contained an active ingredient to be slowly released, while the surface was covered with other active ingredient that could be rapidly delivered. The feasibility of this approach was confirmed through dual loading of dexamethasone in the filament and of prednisolone on the preformed scaffold. Drug-loaded scaffolds were characterized in terms of printability, structural characteristics (DSC, XRD), mechanical properties, biodegradation, and ability to promote cell attachment and proliferation. Finally, anti-inflammatory response and osteoinductive properties were verified in cell cultures.

1. Introduction

The lack of donors and the risk of immune rejection of allografts have prompted an intense research on bone scaffolds that can act as a temporary extracellular matrix, providing structural support to guide cell attachment, proliferation and differentiation [1]. Ideally a bone scaffold must ensure mechanical functionality and stability allowing early postoperative function under physiologic stress conditions, and should have the appropriate porosity range and interconnectivity to guarantee the successful bone ingrowth. Particularly, bone scaffolds with pores larger than 300 μm facilitate the penetration of mineralized tissue and cell migration towards the scaffold center, stimulating nutrient supply and waste products removal [2,3].

Additive manufacturing technologies, and particularly 3D printing, are already launching a revolution in the design, prototyping and fabrication of fully personalized scaffolds, combining image design and internal layering of the 3D structure with micrometer scale resolution, without waste of the usually expensive components [4–6]. Compared to conventional techniques used to produce scaffolds for tissue engineered constructs [7,8], 3D printing has the advantages of more precise pore size and distribution, high levels of interconnectivity, and high mechanical strength [9]. 3D printing allows for easy building objects with virtually any complex architecture, shape or size from a wide variety of materials and with a high degree of precision [1,10,11] following strict quality standards [12].

In the last few years, fused deposition modeling (FDM) 3D printing is attracting a great deal of attention for the design of bone scaffolds from biocompatible, biodegradable polyesters, such as poly(L-lactic

* Corresponding author.
E-mail address: carmen.alvarez.lorenzo@usc.es (C. Alvarez-Lorenzo).
[1] These authors equally contributed to the work.

https://doi.org/10.1016/j.ejpb.2019.05.018
Received 27 March 2019; Received in revised form 17 May 2019; Accepted 17 May 2019
Available online 18 May 2019
0939-6411/

acid) (PLA) [13]. PLA is one of the most widely used materials in clinical applications due to its tunable mechanical properties, degradation into natural metabolites, biocompatibility, and low cost [14,15]. FDM may also enable the use of filaments pre-loaded with bioactive substances, e.g. drugs, which may help tuning the cell behavior or prevent biofilm formation on the final scaffold [16]. The current bottleneck is the reduced choice for materials and the paucity of information about the effects of design and processing variables (during both the hot melt extrusion of the filaments and the 3D printing) on the scaffolds performance [17,18] and, specifically, on drug release pattern [19]. A wide variety of drugs such as antibiotics [20,21], corticosteroids [22,23], and nonsteroidal anti-inflammatory agents [24,25] have been tested to produce drug-eluting 3D printed scaffolds able to improve the regeneration process of the target tissue. In the bone tissue engineering community, there is an on-going research to assess the risk/benefit ratio of corticosteroids for each individual patient. Although long-term treatment with corticosteroids has been often associated with severe bone loss and osteoporosis, the short-term in vivo exposure effects range from localized anti-inflammatory response to substantial, beneficial results on bone regeneration [26]. In particular, prednisolone acts as an anti-inflammatory agent and is also used for the treatment of simple bone cysts in children [27], while the osteoinductive properties of dexamethasone are well known [28,29].

The aim of our work was to elucidate the influence of the mode of incorporation of prednisolone and dexamethasone on the drug release profile from PLA porous bone scaffolds prepared using FDM 3D printing. It should be taken into account that a unique feature of 3D printing is the preparation of personalized scaffolds or tablets. Different patients may require distinct drugs and/or doses. Therefore, instead of starting from a PLA filament preloaded with a given content of drug, in the present study we explored two more versatile strategies to load prednisolone or dexamethasone (Fig. 1). The first strategy that we explored involved the soaking of pieces of PLA filament into a drug solution prepared in a solvent that can reversibly swell PLA facilitating drug diffusion into the filament; subsequent solvent evaporation should render filaments with diameter similar to the initial one, and during 3D printing the melting of PLA may contribute to the efficient incorporation of the drug inside the printed strand. To the best of our knowledge a similar strategy has been only tested to load drugs (fluorescein, aminosalicylic acid, prednisolone) in polyvinyl alcohol filaments to prepare 3D printed tablets [30–32].

The second different strategy consisted in first printing the 3D PLA scaffolds and then soaking the obtained scaffolds into the drug solution in order to exploit that the printed strands have higher specific surface than the PLA filament. Compared to a recently published strategy of loading drugs into porous preformed 3D tablets by soaking into a suspension of drug nanocapsules [33], the combination of the two proposed methods reported in the present study opens the possibility of creating concentration gradients of different drugs in the same scaffold exhibiting distinct release patterns. Namely, the strand core contains an active ingredient to be slowly released, while the surface was covered with other active ingredient that can be rapidly delivered. To test this hypothesis, scaffolds combining both drugs were prepared by loading dexamethasone in the filament and prednisolone on the preformed scaffold (Fig. 1) with the final purpose of achieving, after implantation, a fast anti-inflammatory effect (due to prednisolone release) followed by a sustained osteoinduction (due to dexamethasone release) in the osteoconductive matrix.

All drug-loaded scaffolds were then characterized in terms of printability, structural characteristics, mechanical properties and drug release profile. The effects of the drug incorporation mode on scaffolds stability (in terms of mechanical properties and molecular weight) were also monitored during 4 months storage in a biorelevant medium. Cell tests were conducted to assess the cytocompatibility of the produced 3D printed scaffolds and the ability to promote cell attachment and proliferation. Finally, the anti-inflammatory effect and the osteoinductive properties of the scaffolds were evaluated.

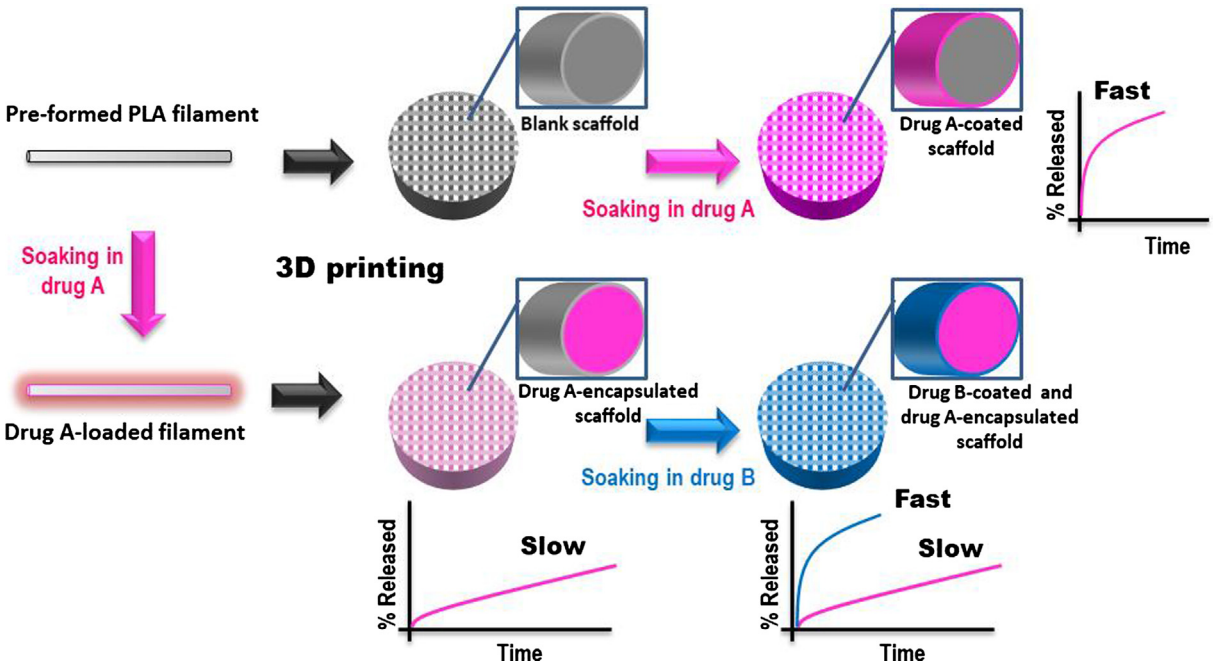

Fig. 1. Strategies to load drugs on either preformed filaments or 3D printed scaffolds. Soaking of preformed 3D printed PLA scaffolds in a drug solution produces strands coated by the drug. Differently, loading of drug A on PLA filaments followed by 3D printing generates scaffolds with the drug A integrated in the strands; subsequent soaking of the drug A-loaded scaffold in drug B solution may give rise to scaffolds with a gradient distribution of the drugs and thus exhibiting different release profiles.

2. Materials and methods

2.1. Materials

Polylactic acid (PLA) in the form of filament for FDM-3D printing was supplied from Createc3D (Createc 3D, Granada, Spain); the PLA MW was determined to be 150,556 Da (PDI 1.14) as described below. Prednisolone was from Sigma (Milan, Italy) and dexamethasone from Fagron (Spain). Methanol was purchased from Scharlab (Spain), ethyl acetate from Merck (Germany) and ethanol from VWR Chemicals (USA). Ultrapure water (resistivity > 18.2 MΩ cm) was obtained by reverse osmosis (MilliQ®, Millipore Spain). All other chemicals and reagents were from Sigma Aldrich (St. Louis MO, USA) and used as supplied.

2.2. Scaffold additive manufacturing

PLA porous scaffolds were prepared using a commercial FDM 3D printer (Regemat3D, Spain). A cylindrical template (.stl file) was designed with Regemat Designer Software and used to print the scaffolds. Object configuration was: diameter = 10 mm, height = 5 mm, pore size = 0.6 mm, layer height = 0.35 mm, and total layers = 14. The infill pattern was diagonal (i.e., linear tilted 45°). The printer was used in its standard configuration, equipped with a nozzle of 0.40 mm in diameter and set at extrusion temperature of 220 °C.

2.3. Drug loading

Prednisolone loading was performed by soaking either raw PLA filaments (length ~ 12 cm) or 3D printed blank scaffolds in prednisolone solution (2.5% w/v) in methanol:ethyl acetate 50:50 vol/vol mixture at 37 °C for 24 h under oscillatory movement. PLA filaments (3 pieces per vial) were placed in test tubes with screw cap containing 28 mL of drug solution to completely cover the filament surface. Separately, the blank scaffolds were incubated in 5 mL of the prednisolone solution (2.5% w/v). The drug-loaded PLA filaments and scaffolds were then dried in oven at 50 °C for 24–48 h.

Prednisolone-loaded PLA filaments were fed into the 3D printer and printed in the form of 3D porous scaffolds as explained above; the obtained scaffolds were named as FPred#S2. Scaffolds loaded with prednisolone after printing raw PLA filament were designated as S2Pred.

Dexamethasone loading was performed as for prednisolone but using 1% (w/v) dexamethasone solution in methanol:ethyl acetate 50:50 vol/vol mixture at 37 °C for 24 h under oscillatory movement. The scaffolds obtained by printing of dexamethasone-loaded filaments were named as FDex#S2. Blank scaffolds that were loaded by soaking in 10 mL dexamethasone solution were designated as S2Dex.

Dually-loaded scaffolds were prepared starting from FDex#S2 scaffolds, which were soaked for 15 min in prednisolone solution (2.5% w/v) in methanol:ethyl acetate 50:50 vol/vol mixture at 37 °C under oscillatory movement. The resultant scaffolds were designated as FDex#S2Pred.

2.4. Drug content evaluation

To assess drug content, three replicates of each drug-loaded scaffold (FPred#S2, S2Pred, FDex#S2 and S2Dex) were immersed, separately, in a volumetric flask with ethanol (5–20 mL). The solution was sonicated for 1–2 h and then incubated under shaking at 37 °C for several days. At given time intervals, 1 mL aliquot was withdrawn from the medium and diluted with 4 mL of water/ethanol 50:50 vol/vol mixture, and the absorbance was recorded at 242 nm for prednisolone and 240 nm for dexamethasone (Agilent 8453 UV/VIS spectrophotometer, Germany). The volume of ethanol removed was replaced with fresh ethanol. The analysis was performed in triplicate.

The content of both dexamethasone and prednisolone in the dually-loaded scaffold FDex#S2Pred was determined using a Waters 996 HPLC with a Sunfire C18 column (3.5 μm, 4.6x150 mm) (Waters, USA). The conditions of the method were: flow 1 mL/min, mobile phase water:-methanol 40:60) and temperature 40 °C [34]. Retention times were 4.8 min for prednisolone and 6.6 min for dexamethasone. Absorbance was measured at 242 nm.

2.5. Dimensional, morphological and topographical analysis

Scaffold diameter and height were measured with a Caliper Digital Electronic (FowlerTM, Newton, Massachusetts). Each measure was performed, at least, in triplicate and results were expressed in terms of mean ± standard deviation (SD). Morphological analysis of the scaffolds was conducted with an Olympus SZ-CTV optical stereo microscope, connected to a JVC TK-S350 video camera (Tokyo, Japan), at 1.5X and 4X magnifications. Details of scaffolds surface topography and 3D architecture were examined using field emission scanning electron microscopy (FESEM Ultra Plus, Zeiss, Oberkochen, Germany). Scaffolds were placed onto metal plates, and 10 nm thick iridium film was sputter-coated (model Q150T-S, Quorum Technologies, Lewes, UK) on the samples before viewing. Some scaffolds were cryofractured in liquid nitrogen to obtain cross-section views.

2.6. Crystalline state

X-ray powder diffraction pattern (XRD) spectra of raw prednisolone and dexamethasone were recorded on a Philips type powder diffractometer fitted with PW1710 control unit, PW1820/00 goniometer and FR590 Enraf Nonius generator, by measuring the scintillation response to Cu Kα radiation versus the 2Θ value over a 2Θ range of 2–40, with a step size of 0.02° and counting time of 2 s per step. The instrument was equipped with a graphite diffracted beam monochromator and copper radiation source ($\lambda(K_{\alpha 1})$ = 1.5406 Å), operating at 40 kV and 30 mA. The XRD spectra of the cylindrical scaffolds were recorded on a Empyrean type diffractometer, equipped with a five-axis goniometer. The X-rays were obtained from a sealed tube of Cu, and the monochromatized radiation with a multilayer mirror optic (W/Si), which makes the incident beam parallel and polarized. This configuration allows for accurate measurements in not-flat samples. The detection of X-rays from the sample was carried out with an area detector PANalytical PIXcel-3D.

Raw materials and blank and drug-loaded scaffolds were also analyzed using a differential scanning calorimeter DSC Q200 (TA Instruments, USA) previously calibrated with indium. The samples were accurately weighed in a 40 μL aluminum pan which was covered, and then heated from 25 to 300 °C at a scanning rate of 10 °C/min in nitrogen atmosphere (50 mL/min). Melting temperature (Tm) and enthalpy (ΔHm) were measured. The analyses were carried out in triplicate. PLA crystallinity was estimated from the difference between the melting (ΔHm) and the cold crystallization (ΔHcc) enthalpies referred to the melting enthalpy of 100% crystalline PLA (ΔH_{100} = 93.1 J/g [35]), as follows [36]

$$Crystallinity\ \ (\%) = \frac{\Delta Hm - \Delta Hcc}{\Delta Hm_{100} \cdot m_{PLA}} \times 100 \quad (1)$$

In this equation, m_{PLA} represents the weight fraction of PLA in the scaffold.

The porosity of the scaffolds was calculated as

$$Porosity\ \ (\%) = \left(1 - \frac{d_{envelop}}{d_{PLA}}\right) \times 100 \quad (2)$$

In this equation, d_{app} represents the envelop density of the scaffold (weight/apparent volume) and d_{PLA} represents the skeletal density of PLA.

2.7. Mechanical properties

Mechanical properties of 3D printed scaffolds were investigated using a TA.XT plus Texture Analyzer (Stable Micro Systems, Surrey, UK) equipped with a 30 Kgf (~294 N) load cell. Scaffolds underwent 10 successive stress-strain cycles applying a Cycle Until Count mode, which consisted in recording the stress-strain curves of the cylinders when subjected to uniaxial compression along their short axis (height) by downward movement (0.5 mm/s) of an aluminum cylinder probe (20 mm) until a stress of 196 N. The activation strength was set at 1 g. Force and deformation were measured and later converted to engineered stress and strain using the initial dimensions of the scaffold and its deformation under pressure [37]. Young's modulus was calculated as the slope of the linear (elastic) region of the stress-strain curve [38]. The hardness was estimated as the peak force value, and the compressibility was calculated from the area under the force-distance plot. Mechanical behavior of scaffolds was also evaluated by applying the force along the diameter during 10 successive stress-strain cycles. Scaffolds of each formulation type were stored for 31, 66 and 120 days in phosphate buffered saline (PBS) pH 7.4 at 37 °C and then re-evaluated regarding mechanical properties.

2.8. Drug release experiments

Drug release studies were carried out, in triplicate, in PBS pH 7.4 medium under sink conditions (10–20 mL) using an incubating shaker at 37 °C and 200 rpm. At pre-determined times, 1 mL samples of the release medium were taken, and the drug concentration was quantified from absorbance measurements at 247 nm for prednisolone and 242 nm for dexamethasone (Agilent 8453 UV/vis spectrophotometer, Ratingen, Germany). Then, the samples were returned to the corresponding vials.

In parallel, release experiments from all scaffolds including FDex#S2Pred were also carried out, in triplicate, in PBS/ethanol 30/70 vol/vol medium (10 mL), which may simulate the usual serum supplemented release medium (PBS with 10% fetal bovine serum) but avoiding the presence of proteins [39]. At predetermined times along four months, 1 mL of medium was withdrawn to measure drug release and replaced with 1 mL of fresh medium. The release of both drugs was quantified using a Waters 996 HPLC with a Sunfire C18 column (3.5 μm, 4.6 × 150 mm) (Waters, USA). The conditions of the method were: flow 1 mL/min, mobile phase water:methanol (40:60 vol/vol) and temperature 40 °C [34]. The absorbances were measured at 242 nm.

2.9. Biodegradation monitoring

Molecular weight of raw PLA filament, freshly prepared blank scaffolds, and scaffolds that had being incubated in PBS release medium for 66 days was quantified using an HPLC-GPC (Waters, USA) fitted with a Styragel column HR 4E, 5 μm, 7.8 × 300 nm (50–100 KDa; Waters) and photodiode array detector. Scaffolds were removed from the release medium, carefully washed with water and then dried. All specimens were dissolved in THF at a concentration of 1%(w/v) applying gentle stirring and heating (35–40 °C). The injection volume was 30 μL and the run time was 12 min. Data were recorded at 230 nm and analysed using Empower 3 software and a Log Molecular Wt vs. retention time calibration curve. Additionally, mechanical properties of the incubated scaffolds were recorded again as explained above.

After 120 days in the release test medium, scaffolds were removed, washed with water, wiped with filter paper and weighed. Then, the scaffolds were freeze-dried, weighed again and the mechanical properties, SEM and optical stereo images, and DSC analysis recorded again.

2.10. Cytotoxicity test

In vitro cytotoxicity of 3D printed PLA scaffolds was evaluated using murine fibroblasts (CCL-163, ATCC, USA) and applying two different assays (LDH and WST-1). Cell line was cultured in αMEM (89%), supplemented with 10% FBS and 1% penicillin (10,000 UI/mL)/streptomycin (10,000 μg/mL). Briefly cells were seeded in 24-well plates with 0.5 mL of culture medium (20,000 cells/well) and grown for 24 h at 37 °C (95% RH and 5% CO_2) for achieving confluence. After 24 h, previously sterilized scaffolds (by soaking in ethanol 70% for few seconds and then allowing the ethanol to completely evaporate) were brought into the wells and put in contact with cells for 48 h at 37 °C/5% CO_2. Controls included cells without treatment and cells treated with 0.7 mM and 7 mM prednisolone (maximum drug concentrations provided to the cell culture medium by the scaffolds FPred#S2 and S2Pred, respectively) or 0.1 mM and 1 mM dexamethasone (maximum drug concentrations provided by the scaffolds FDex#S2 and S2Dex, respectively). For LDH assay, aliquots of medium (100 μL) were taken and mixed with the reaction medium (100 μL) provided with the Cytotoxicity Detection KitPlus (LDH, Roche). The plates were incubated for 10 min at 15–25 °C protected from light. The absorbance at 490 nm was immediately measured (UV Bio-Rad Model 680 microplate reader, USA). The experiments were carried out in triplicate and cytotoxicity was calculated as follows:

$$Cytotoxicity\ \ (\%) = \frac{Abs_{exp} - Abs_{negative\ \ control}}{Abs_{positive\ \ control} - Abs_{negative\ \ control}} \cdot 100 \quad (3)$$

Cell proliferation was evaluated using the WST-1 reagent (Roche, Switzerland). After 48 h in cell culture, scaffolds were removed from the wells, and the cell proliferation assay was carried out following manufacturer instructions. Absorbance was read at 450 nm (UV Bio-Rad Model 680 microplate reader, USA). The experiments were carried out in triplicate and cell viability (%) was calculated using the following equation:

$$Cell\ \ viability\ \ (\%) = \frac{Abs_{exp}}{Abs_{negativecontrol}} \cdot 100 \quad (4)$$

2.11. Anti-inflammatory response

The anti-inflammatory activity of drug-loaded scaffolds was evaluated in lipopolysaccharide (LPS)-challenged macrophages (Raw 264.7, ATCC® TIB-71™) monitoring PEG_2 and TNFα response. Macrophages were expanded in DMEM supplemented with 10% FBS and 1% penicillin/streptomycin at 37 °C (95% RH and 5% CO_2). Scaffolds were placed in 24-well plates, seeded with 200,000 cells per well and stimulated after 24 h of culture with LPS at a 100 ng/mL final concentration [40]. The anti-inflammatory activity normalized by DNA was evaluated after 48 h of culture in terms of TNF-α and PGE2 secretion. Cell culture supernatants were collected and used to perform an ELISA to analyze TNF-α expression (Invitrogen) and an EIA to quantify PGE2 (Arbor) following manufacturers' protocol. Cells were then washed with DPBS for 5 min after which 0.4 mL of cell lysis buffer was added to each well (1% SDS, 1 mM EDTA and 10 mM Tris-HCl at pH 8). The obtained cell lysates, after 5 min incubation with lysis buffer at room temperature, were used to measure total DNA content with a Quant-iT™ PicoGreen® dsDNA Kit (Thermo Fisher Scientific PicoGreen) according to manufacturers' protocol. The sample fluorescence was measured in a FLUOstar OPTIMA microplate reader (BMG Labtech, USA) (λ_{exc} 480 nm; λ_{em} 520 nm).

2.12. Osteogenic activity

The osteogenic effect of blank scaffolds, S2Dex, FDex#S2 and FDex#S2Pred scaffolds was evaluated using human mesenchymal stem cells derived from bone marrow (hMSC; ATCC PCS-500-012). hMSCs were cultured in a 175 cm^2 cell culture flask with 20 mL of αMEM (84%) supplemented with FBS HI (15%) and antibiotics (penicillin

10.000 UI/mL, streptomycin 10.000 μg/mL; 1%) until 80% confluence was reached. Then, the cells were trypsinized with 10 mL Trypsin-EDTA 0.25%. Scaffolds were soaked in ethanol 70% for few seconds, placed in 24-well plates and allowed the ethanol completely evaporated. Then, cells were seeded on the scaffold surface by depositing 100 μL of the cell suspension (250,000 cells/mL) on each side of the scaffold and waiting 30 min between seedings to allow cell attachment (50,000 cells per well). Cell-seeded scaffolds were incubated for 21 days (37 °C, 95% RH, 5% CO_2) in 1 mL of DMEM (89%) supplemented with FBS HI (10%) and antibiotics (penicillin 10,000 UI/mL, streptomycin 10.000 μg/mL, fungizone 25 μg/mL; 1%). The osteogenic effect was evaluated after 3, 7 and 14 days recording ALP activity and osteocalcin. Negative controls were prepared as explained above without scaffolds. Positive controls were cells cultured in osteogenic medium composed of DMEM (89%) supplemented with FBS (10%), antibiotics (penicillin 10.000 UI/mL, streptomycin 10.000 μg/mL, fungizone 25 μg/mL; 1%), β-glycerol phosphate (10 mM), ascorbic acid (50 μM) and dexamethasone (100 nM). Culture media were replaced every two days. All scaffolds were tested in quadruplicate at four time points. Supernatants and cell lysates were collected at days 3, 7, 14 and 21. Cells were lysated by addition of Tris-HCl 10 mM + 0.1% Triton X-100 (1.5 mL for samples (0.75 mL for cells on the bottom-well + 0.75 mL for cells in the scaffolds) and 0.75 mL for negative and positive controls). Both supernatants and cell lysates were kept at −150 °C until their analysis.

To carry out the alkaline phosphatase (ALP) test, cell lysates were exposed to three freezing (−80 °C)/thawing cycles (45 min per cycle). Lysates were cleared by centrifugation at 5000 rpm (5200g; Megafuge 1.0R, Heraeus, Germany) for 15 min at 4 °C. p-N-phenyl-phosphate substrate (18.6 mg) was dissolved in $MgCl_2$/AMP buffer (10 mM, 10 mL). This substrate solution (100 μL) was mixed with test solution (40 μL cell lysate and 60 μL deionized water) and incubated at 37 °C for 1 h. The reaction was stopped by adding 100 μL of 0.3 M NaOH, the absorbance measured at 440 nm, and the results compared to those obtained with 4-nitrophenol standard solutions. Total DNA content was quantified using a Quant-iT™ PicoGreen® dsDNA Kit as explained above.

Human Osteocalcin assay was carried out following the Human Osteocalcin Quantikine ELISA Kit protocol (R&D Systems, USA). The optical density was measured at 440 nm. Results were normalized by the DNA content.

Cell morphology was observed for hMSCs cultured on the scaffolds for 14 days as explained above. After 14 days incubation, the scaffolds were washed twice with PBS, fixed with 4% paraformaldehyde solution, and the cell nuclei and membrane were stained using 4,6-diamidino-2-phenylindole and Alexa fluor 488 dye, respectively. Micrographs were acquired using a Confocal Spectral Microscope Leica TCS-SP5 (LEICA Microsystems Heidelberg GmbH, Mannheim, Germany).

2.13. Statistical analysis

Effects of scaffolds composition on anti-inflammatory response and osteogenic activity at each time point were analyzed using ANOVA and multiple range test (Statgraphics Centurion XVI 1.15, StatPoint Technologies Inc., Warrenton VA).

3. Results and discussion

3.1. Scaffold additive manufacturing and drug loading

3D scaffolds loaded with prednisolone and dexamethasone were prepared by means of FDM 3D printing using two different strategies that involved either starting from the loading of preformed PLA filaments which were then printed, or first printing the scaffold for the subsequent loading of the drug (Fig. 1). Both prednisolone and dexamethasone are crystalline drugs (Fig. 2). Prednisolone solubility in water has been reported to be 223 mg/L [41] and its melting

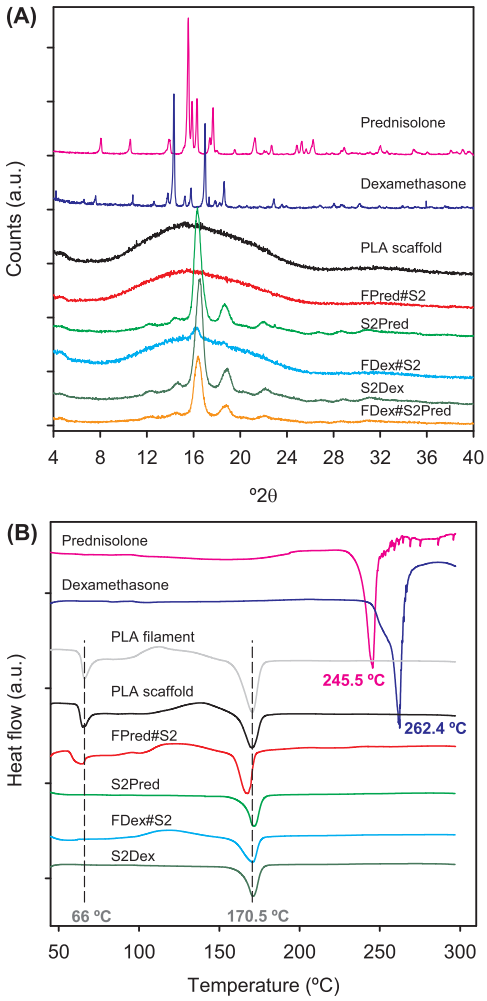

Fig. 2. XRD spectra (A) and DSC scans (B) of raw materials, blank scaffolds, scaffolds made of drug-loaded filaments (FPred#S2 and FDex#S2) and scaffolds loaded after 3D printing (S2Pred and S2Dex). XRD spectrum of dually-loaded scaffolds (FDex#S2Pred) is also shown.

temperature was 245.5 °C (Fig. 2) in good agreement with literature. Dexamethasone solubility is slightly lower (~100 mg/L) [41] and its melting temperature was 262.4 °C (Fig. 2), also in agreement with previously published data [42]. At higher temperature both drugs rapidly decompose. Therefore, the additive manufacture processing should minimize the exposure of these drugs to high temperature for prolonged time to avoid stability problems. Thus, from a technological perspective our strategy of post-loading of either preformed PLA filaments or final scaffolds has the two-fold aim of (i) being more versatile regarding personalized medicine, since blank filaments or scaffolds could be prepared in advance and, once required, they could be loaded with the adequate drug at the needed dose and showing the required release profile; and (ii) better preserving drug stability by avoiding the exposition of the drugs to harsh conditions during hot melt extrusion of the filaments and minimizing the time at high temperature during 3D printing, i.e., few seconds at 220 °C. It should be noted that the semi-crystalline PLA used melted at 170.5 °C (Fig. 2).

Drug loading of PLA filament was performed using a versatile method that relies on the selection of a solvent that is able to reversibly swell PLA (without dissolving it) and at the same time can solubilize the selected drug. It is expected that the drug passively diffuses into the swollen polymer matrix and is trapped during the drying phase, as previously observed for polyvinyl alcohol filaments soaked in ethanolic drug solutions [30–32]. Based on literature data [43], several

preliminary swelling experiments were performed on PLA filament using ethanol, methanol, ethyl acetate, o-xylene and di-n-butyl phthalate, and drug concentrations ranging from 0.5 to 5% w/v according to the solubility in each solvent. Ethyl acetate and o-xylene showed high ability to swell the polymer, but poor ability to solubilize the drugs; di-n-butyl phthalate exhibited deficient capability in both PLA swelling and drug solubilization. Ethanol and methanol showed limited swelling ability, but good drug solubilization. Thus, a methanol:ethyl acetate 50:50 vol/vol mixture was selected as soaking solution and the drug concentration was set at 2.5% (w/v) for prednisolone loading and at 1% (w/v) for dexamethasone loading. Desirable loading of dexamethasone is in the 0.01–1% range, i.e. 0.1–10 mg per gram of scaffold; higher contents may cause untoward systemic effects [44]. The amount loaded could be tuned by changing drug concentration in the swelling medium and the time of loading. In the case of prednisolone, the inhibition of mixed lymphocyte reactions has been shown to occur at total plasma concentrations of ~0.2 mg/L [45]. Therefore, a scaffold piece of 100 mg should contain at least 0.2 mg (i.e., > 2 mg per gram).

The drug-loaded PLA filaments were then dried and used as feed for 3D printing. After drug loading process (soaking/drying), PLA filaments resulted to be whitish, with a smooth outer surface and showed a slight increase in diameter (~8–10%), but despite that they were easily extruded by the printer in the form of 3D pore-defined scaffolds (FPred#S2 and FDex#S2).

Several blank (S) and drug-loaded scaffolds (FPred#S2 and FDex#S2) were prepared using the selected printing parameters and starting from either raw PLA filaments or drug-loaded PLA filaments, respectively. Some blank scaffolds were loaded after printing by soaking in the drug solution prepared in methanol:ethyl acetate 50:50 vol/vol mixture (as for the filaments) obtaining S2Pred and S2Dex. It should be noted that previous reports on 3D printing of prednisolone-loaded polyvinyl alcohol filaments used a nozzle temperature of 230 °C, i.e. 10 °C above the one we applied, and the drug was still stable [32]. In the case of dexamethasone, exposition at 185 °C for 5 min during hot melt extrusion did not cause detrimental effects [42].

Dually-loaded FDex#S2Pred were prepared by soaking of FDex#S2 scaffolds in prednisolone solution. The soaking time was carefully adjusted by monitoring prednisolone loading and dexamethasone discharge; an adequate balance was obtained applying 15 min soaking. This protocol allowed for achieving prednisolone loads still relatively high (ca. 11 mg/g) compared to those obtained with blank scaffolds soaked for 24 h (approx. 16 mg/g), while dexamethasone content was still in the therapeutic range. Weight and dimensions of the blank and all drug-loaded scaffolds are summarized in Table 1. From the dimensions and assuming that the skeletal density of PLA is ca. 1.3 g/cm^3 [46], the porosity of the scaffolds was calculated (using Eq. (2)) to be close to 60%.

As reported in Table 1, drug content was ca. 0.26 (s.d. 0.01)% w/w for FPred#S2 scaffolds and of 0.09 (s.d. 0.01)% w/w for FDex#S2 scaffolds, which were printed starting from prednisolone- or dexamethasone-loaded PLA filament respectively. Differently, drug loading was 1.62 (s.d. 0.17)% w/w for S2Pred scaffolds and 0.35 (s.d. 0.04)% w/w for S2Dex scaffolds, which were loaded with the drug after 3D printing. The higher drug content of scaffolds loaded after printing compared to those scaffolds formed by drug-loaded filaments is explained by the fact that PLA strands of scaffolds loaded after printing are thinner (approx. 0.4 mm) than pristine PLA filament (1.75 mm in diameter) and they can expose much higher surface area to the loading solution, which in turn should facilitate drug diffusion into the PLA matrix.

3.2. Morphology, surface topography and 3D architecture

Among the produced scaffolds, there were no significant differences in terms of diameter and height (Table 1). As shown by stereomicroscopy images (Fig. 3), the produced scaffolds had size and shape close to that programmed by the software, which confirmed the reproducibility of the 3D printed scaffolds. Main difference was seen in the color of the scaffolds: transparent for the blank (non-loaded) ones, translucent for FPred#S2 and FDex#S2, and whitish for S2Pred, S2Dex, and FDex#S2Pred.

FESEM analysis allowed investigating in detail the surface topography and 3D architecture of the scaffolds (Fig. 4). All scaffolds were composed of 0.35–0.40 mm struts forming 0.6 mm horizontal square pores. The horizontal layers of struts were vertically deposited in 0.35 mm superimposition increments. The micrographs of FPred#S2 and FDex#S2 scaffolds revealed fiber diameters thinner than those shown by 3D printed scaffolds of raw PLA filament. Moreover, the surface of scaffolds prepared from drug-loaded PLA filaments showed abundant and deep micropores, but no signal of drug crystals was observed. Differently, S2Pred and S2Dex scaffolds were formed by more uniform strands which did not show pores. Their surface appeared rough and completely covered by a high amount of drug crystals. These findings indicate that the step at which the drug loading occurs notably determines the appearance and the morphology of the strands. During the 3D printing the PLA of drug-loaded PLA filaments melts and may solubilize the drug deposited on the surface; a solid solution may be obtained when cool down. According to Fig. 2, printing temperature (220 °C) was above PLA melting temperature but below the melting temperature of the drugs. Evaporation of traces of residual solvent during the melting in the nozzle may be responsible for the enhanced pore formation (compared to non-loaded filaments), as observed during conventional hot melt extrusion [47]. Differently, scaffolds loaded after printing contained most drug at the surface of the strands, which crystallizes during slow solvent evaporation. Interestingly, FDex#S2Pred scaffolds showed a nice fidelity with the 3D design and had strands with few pores and the surface completely coated with prednisolone particles.

3.3. Crystallinity

XRD spectra (Fig. 2a) confirmed the absence of crystalline peaks in

Table 1
Weight, drug loaded, diameter and height of PLA scaffolds prepared using FMD 3D printing: blank scaffold (S), scaffolds prepared from prednisolone-loaded filament (FPred#S2) or dexamethasone-loaded filament (FDex#S2), scaffolds loaded by soaking in prednisolone solution (S2Pred) or dexamethasone solution (S2Dex), and the dually-loaded scaffolds (FDex#S2Pred) (n = 3, mean values and, in parenthesis, standard deviations).

Scaffold	Weight (mg)	Drug loaded (mg/g)	Diameter (mm)	Height (mm)	Porosity
S	141.1 (2.5)	/	10.35 (0.15)	4.45 (0.09)	0.71
FPred#S2	157.7 (2.8)	2.59 (0.14)	10.48 (0.12)	4.49 (0.05)	0.69
S2Pred	145.8 (1.3)	16.24 (1.72)	9.71 (0.12)	4.31 (0.04)	0.65
FDex#S2	155.0 (4.9)	0.85 (0.14)	10.37 (0.11)	4.48 (0.11)	0.68
S2Dex	146.2 (2.5)	3.50 (0.35)	9.74 (0.05)	4.35 (0.04)	0.65
FDex#S2Pred	161.4 (2.3)	10.91 (1.53)[a]/0.11 (0.03)[b]	9.75 (0.07)	4.45 (0.04)	0.66

[a] Prednisolone loading.
[b] Dexamethasone loading.

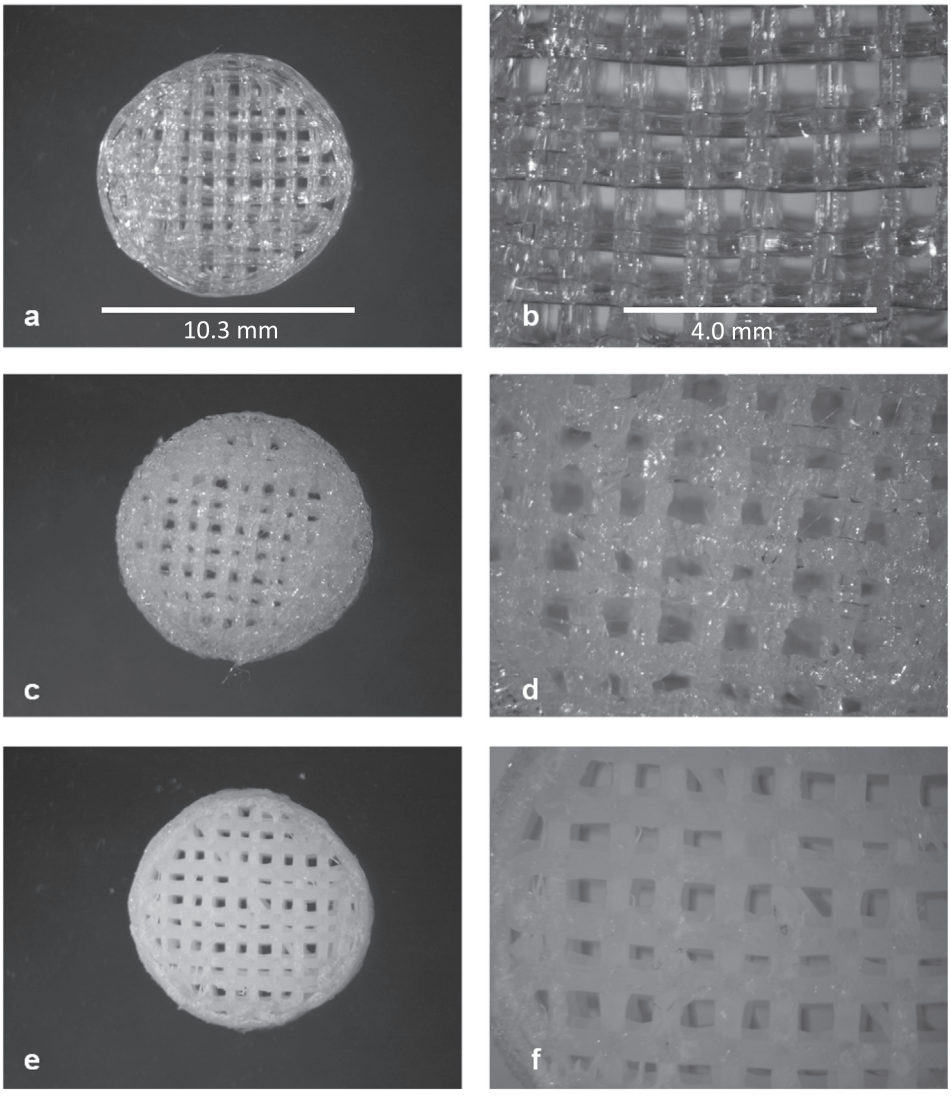

Fig. 3. Stereomicroscopy images of scaffolds at 1.5× and 4× magnifications: (a–b) blank, (c–d) FPred#S2, and (e–f) S2Pred scaffolds.

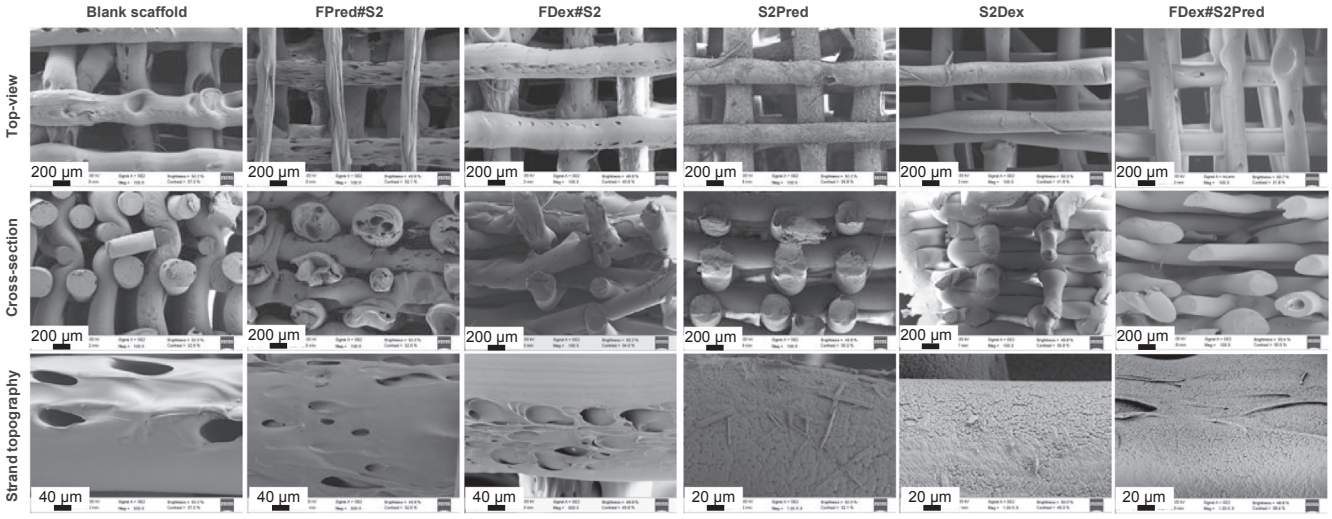

Fig. 4. FESEM micrographs of PLA scaffolds prepared using FMD 3D printing: blank scaffold (S), scaffolds prepared from prednisolone-loaded filament (FPred#S2) or dexamethasone-loaded filament (FDex#S2), scaffolds loaded by soaking in prednisolone (S2Pred) or dexamethasone (S2Dex) solution, and the dually-loaded scaffolds (FDex#S2Pred). Top-view and cross-section were recorded at 100X magnification (scale bar 200 µm); strand topography was visualized at 500X (blank scaffold, FPred#S2 and FDex#S2; scale bar 40 µm) and 1000× (S2Pred, S2Dex and FDex#S2Pred; scale bar 20 µm).

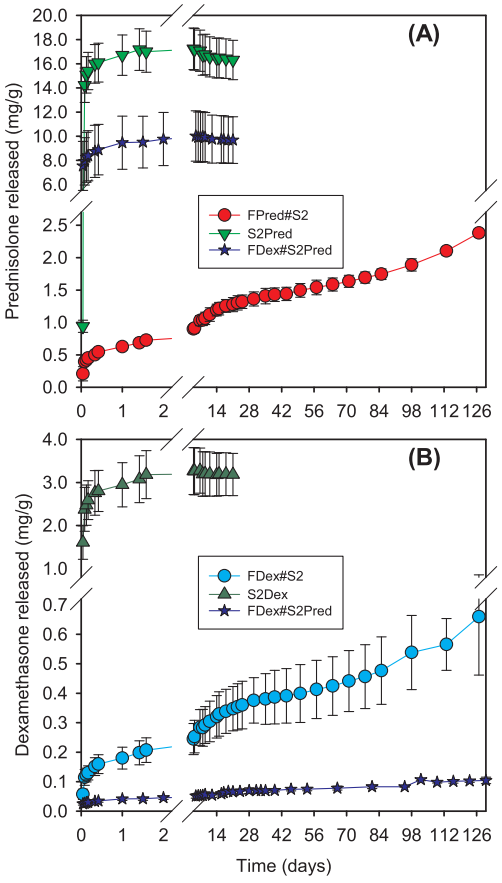

Fig. 5. (A) Prednisolone release profiles in PBS/ethanol 30:70 vol/vol from scaffolds made of drug-loaded filaments (FPred#S2), scaffolds loaded after 3D printing (S2Pred) and dually-loaded scaffolds (FDex#S2Pred). (B) Dexamethasone release profiles in PBS/ethanol 30:70 vol/vol from scaffolds made of drug-loaded filaments (FDex#S2), scaffolds loaded after 3D printing (S2Dex) and dually-loaded scaffolds (FDex#S2Pred).

FPred#S2 and FDex#S2, and their patterns were similar to those of blank PLA scaffold. Differently, S2Pred and S2Dex showed some crystalline peaks in good agreement with the SEM micrographs. XRD scans of FDex#S2Pred were superimposable with those of S2Pred, confirming the presence of prednisolone crystalline particles at the scaffold surface.

To gain further insight into the crystallinity of both the scaffold and the drugs, DSC scans of the drugs, blank PLA filament and scaffold, and drug-loaded scaffolds were recorded (Fig. 2b). PLA filaments and scaffolds were characterized by multiphase transitions, involving a glass transition with an endothermic event (~66 °C), a cold crystallization (~110–120 °C) and a final melting (~170.5 °C), in agreement with previous reports on pure PLA systems [48]. Blank 3D printed PLA scaffold behaved as the blank PLA filament with the exception of the shift of the cold crystallization peak towards higher temperature in the case of the scaffold. Enthalpies associated to cold crystallization (~19 J/g) and final melting (~30 J/g) of blank PLA filament and scaffold were similar, and revealed PLA crystallinity values of 11.8%. Relevantly those scaffolds prepared from drug-loaded filaments showed a small decrease in the glass transition temperature (3 °C lower) compared to blank PLA scaffolds, which suggests a plasticizing effect of the drug. This phenomenon was particularly evident in the case of prednisolone-loaded scaffolds due to the higher content in drug compared to the dexamethasone-loaded scaffolds. Also relevantly, S2Pred and S2Dex showed a minimized cold crystallization and increased melting enthalpy (35–36 J/g), which suggests that PLA underwent an increase in crystallinity after partial swelling in the organic solvents followed by slow evaporation. FDex#S2Pred behaved as S2Pred. Relevantly, drug melting peaks were not observed for any scaffold, not even for S2Pred, S2Dex or FDex#S2Pred in spite they clearly exhibited drug crystals on their surface. The reason for this finding can be that the melting of PLA during the DSC analysis causes the drug crystals on the strand surface to dissolve, which also explains the lack of peaks in the XRD spectra of scaffolds prepared with drug-loaded filaments. This hypothesis relies on that the amount of drug on the surface is sufficiently low to allow complete dissolution in melted PLA in a short time period. Previous reports on implants prepared by hot melt extrusion of PLA:dexamethasone 50:50%(w/v) showed DSC scans in which the melting of the crystalline drug was still evident, but the drug melting peak disappeared for implants prepared with 90:10%(w/v) mixtures [42]. This previous report also avails the hypothesis of that both prednisolone and dexamethasone on the surface of PLA filaments can dissolve in melted PLA during the 3D printing becoming dispersed at molecular level into the strands.

3.4. Mechanical properties

Mechanical behavior of the manufactured scaffolds was assessed by recording the stress-strain curves during 10 successive cycles of compression with a load of 196N on the larger surface (Fig. S1 in Supporting Information file). The response was perfectly elastic; the minor deformation observed under pressure was completely recovered during the recovery steps, and thus the deformation-recovery profiles were symmetrical during the 10 cycles for all the scaffolds tested (see detail for FDex#S2Pred scaffold in Fig. S1). No cracks in the strands were observed after the successive deformations. All scaffolds showed Young's modulus in the range of 12 to 14 MPa, which is quite close to the Young's modulus of human cancellous bone [49]. This means that the observed differences in strand porosity and thickness have no relevant repercussion on the mechanical behavior of the scaffold as a whole.

Interestingly, the scaffolds showed noticeable anisotropy. When the force was applied along the diameter, the scaffold became irreversibly deformed (ca. 50% decrease in diameter) in the first stress-strain cycle although no further deformation was observed during the subsequent 9 cycles.

3.5. Drug release profiles

Drug-loaded scaffolds were tested to verify whether the PLA matrix was able to control and modulate drug release. Preliminary experiments were carried out in PBS under sink conditions (Fig. S2 in Supporting Information file). FPred#S2 and FDex#S2 scaffolds prepared with loaded filaments showed very sustained drug release, with less than 10% released in the first two weeks. This finding corroborates the efficient incorporation of the drug inside the filament during the printing process. Differently, S2Pred and S2Dex, loaded after printing, showed a burst release of ca. 50% of the drug in the first 6 h, in good agreement with the localization of the drug on the scaffold surface.

The drug release test was also carried out in PBS supplemented with 70% vol/vol of ethanol in order to simulate the usual serum-supplemented medium that mimics in vivo conditions [50]. For the sake of comparison release profiles of prednisolone and dexamethasone are depicted in different plots in Fig. 5. FPred#S2 and FDex#S2 prepared with drug-loaded filaments provided sustained release for more than four months, while scaffolds S2Pred and S2Dex loaded after printing delivered ~80% drug in the first day, followed by the sustained release of the remaining dose along one week. Release profiles in percentage can be seen in Fig. S3 (Supporting Information).

Dually-loaded scaffolds made of dexamethasone-loaded filaments and then coated with prednisolone after printing (FDex#S2Pred) were also investigated. To prepare these scaffolds, the filaments were soaked in dexamethasone solution as for the preparation of FDex#S2, and then the 3D printed scaffolds were placed for 15 min in a prednisolone

solution in methanol:ethyl acetate mixture. As expected, the dually loaded FDex#S2Pred released quite fast the prednisolone loaded showing ~80% burst release in the first 24 h and achieving 100% release in one week (blue stars in Fig. 5A and S3). Differently, they sustainedly delivered dexamethasone for four months (blue stars in Fig. 5B and S3). Compared to FDex#S2, the dually-loaded scaffolds released less dexamethasone because of drug leakage during the loading of prednisolone, but the release profiles showed the same pattern (Fig. S3).

3.6. Biodegradation monitoring

Scaffolds were maintained for two months in the PBS release medium, carefully washed and reevaluated regarding mass, molecular weight, and mechanical properties. The weight loss due to drug release and polymer erosion was below 5% in all cases after 66 days soaking. However, the molecular weight notably decreased from 150,556 Da (PDI 1.14) of raw PLA filament and freshly printed scaffolds, to 71,360 Da (PDI 2.04) of control non-loaded scaffolds, 78,056 Da (PDI 1.89) of scaffolds made of drug-loaded filaments, and 70,055 Da (PDI 2.10) of drug-loaded post-printed scaffolds. Thus, the molecular weight roughly decreased to the 50% of the initial value in the first 2 months. This value agrees well with the evolution of the molecular weight of PLA under in vivo conditions [51]. Interestingly, no significant changes were recorded in the mechanical properties of the scaffolds, which means that PLA molecular weight is still sufficiently large and the scaffolds can still perform as suitable bone scaffolds.

After 4 months in the release medium, the scaffolds still maintained their structure without apparent changes (Fig. S4 in Supporting Information). Changes in overall diameter and height were below 2% compared to pristine printed scaffolds. The total weight lost was around 5% for FPred#S2 and FDex#S2, but up to 13% for S2Pred, S2Dex and FDex#S2Pred. The mechanical properties also showed remarkable changes. The Young's modulus of S2Pred and S2Dex decreased to 2–4 MPa in the first tension cycle and the scaffolds broke in small pieces at a force below 196 N. Control PLA scaffolds (without any drug) had Young's modulus of 6.7 MPa, but also broke in the first cycle. Differently, FPred#S2 and FDex#S2 scaffolds showed the highest Young's modulus (in the 9–10 MPa range). The FDex#S2Pred scaffolds showed an intermediate behavior with Young's modulus of ca. 9 MPa, but a breaking force of also 196 N.

These findings point out that the loading protocol may alter the long-term mechanical properties. Specifically, S2Pred and S2Dex (loaded after printing) rapidly released the drug and thus exposed the PLA filament to the medium. Differently, FPred#S2 and FDex#S2 that loaded the drugs in the PLA matrix during printing showed an efficient sustained release, as observed in Fig. 5. Since the drugs are quite hydrophobic, they do not facilitate the entrance of the aqueous medium in PLA structure which may contribute to a better maintenance of the mechanical properties. Relevantly, drug release rate from FPred#S2 and FDex#S2 accelerated in the 2–4 months time interval, in good correlation with the decrease in molecular weight.

3.7. Cytocompatibility and anti-inflammatory activity

Before challenging the scaffolds regarding their capability to inhibit inflammatory response and to induce bone regeneration, scaffolds cytocompatibility was first screened using fibroblast cells because of their sensitiveness to any toxic substance. Both LDH cytotoxicity test and WST-1 cell proliferation test after 48 h of direct contact revealed adequate cytocompatibility. LDH test showed cytotoxicity values below 8%. Except S2Pred and S2Dex, all scaffolds led to cell proliferation levels similar to those recorded for cells growing in the absence of the scaffolds (negative control) (Fig. S5 in Supporting Information file). As observed for the release test in PBS, S2Pred and S2Dex are expected to deliver quite rapidly a relevant percentage of the drug loaded towards the cell culture medium. Indeed, the low cell proliferation values of S2Dex agreed quite well with those recorded for free dexamethasone (1 mM) dispersed in the cell culture medium. Nevertheless, cell proliferation recorded for both S2Pred and S2Dex was still above 65%.

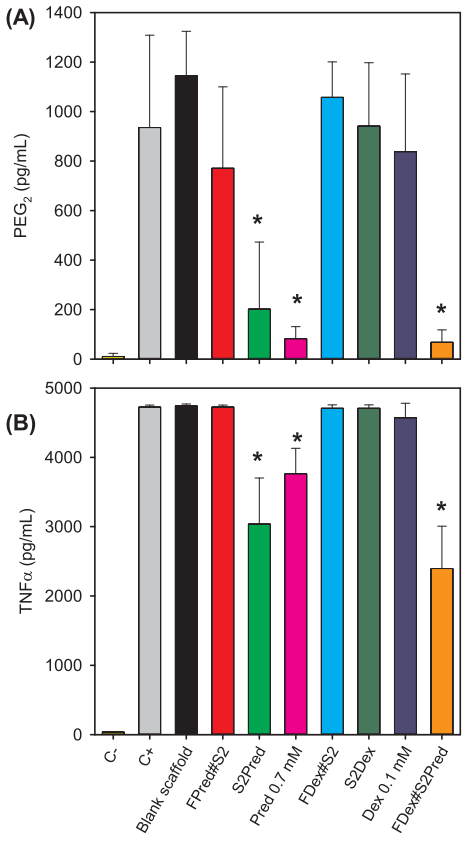

Fig. 6. PEG_2 and TNF-α levels (pg/mL) released by macrophages incubated with the scaffolds and stimulated with lipopolysaccharide (LPS). Negative control refers to non-stimulated cells, while positive control refers to stimulated macrophage cells. *Statistically significant differences with the positive control (ANOVA and multiple range test $p < 0.05$; n = 3). The codes are as follows. Blank scaffold: 3D printed scaffold without drug. FPred#S2: scaffolds made of prednisolone-loaded filaments. S2Pred: scaffolds loaded with prednisolone after 3D printing. Pred 0.7 mM: prednisolone (0.7 mM) solution. FDex#S2: scaffolds made of dexamethasone-loaded filaments. S2Dex: scaffolds loaded with dexamethasone after 3D printing. Dex 0.1 mM: dexamethasone (0.1 mM) solution. FDex#S2Pred: dually-loaded scaffolds.

The capability of the scaffolds to attenuate an inflammatory response was challenged against macrophages stimulated using LPS (Fig. 6). Blank scaffolds did not attenuate the levels of PEG2 and TNFα, which were similar to those obtained for the positive control. Differently, all scaffolds loaded with prednisolone on the surface, namely S2Pred and FDex#S2Pred caused a notable decrease in the PEG2 and TNFα levels, being as efficient as the free drug dispersed in the cell culture medium (ANOVA $p < 0.001$; multiple range test $p < 0.05$). Differently, dexamethasone-loaded scaffolds did not significantly modify the inflammatory response in good agreement with the results recorded for dexamethasone directly added to the medium. Thus, loading of prednisolone on the scaffold surface may allow tuning the post-implantation inflammatory response into adequate levels for bone regeneration [52].

3.8. Osteogenic activity

Finally, the scaffolds were challenged regarding capability to induce differentiation of mesenchymal stem cells (hMSCs) to osteoblast. Osteocalcin and ALP activity were monitored (Fig. 7A and B).

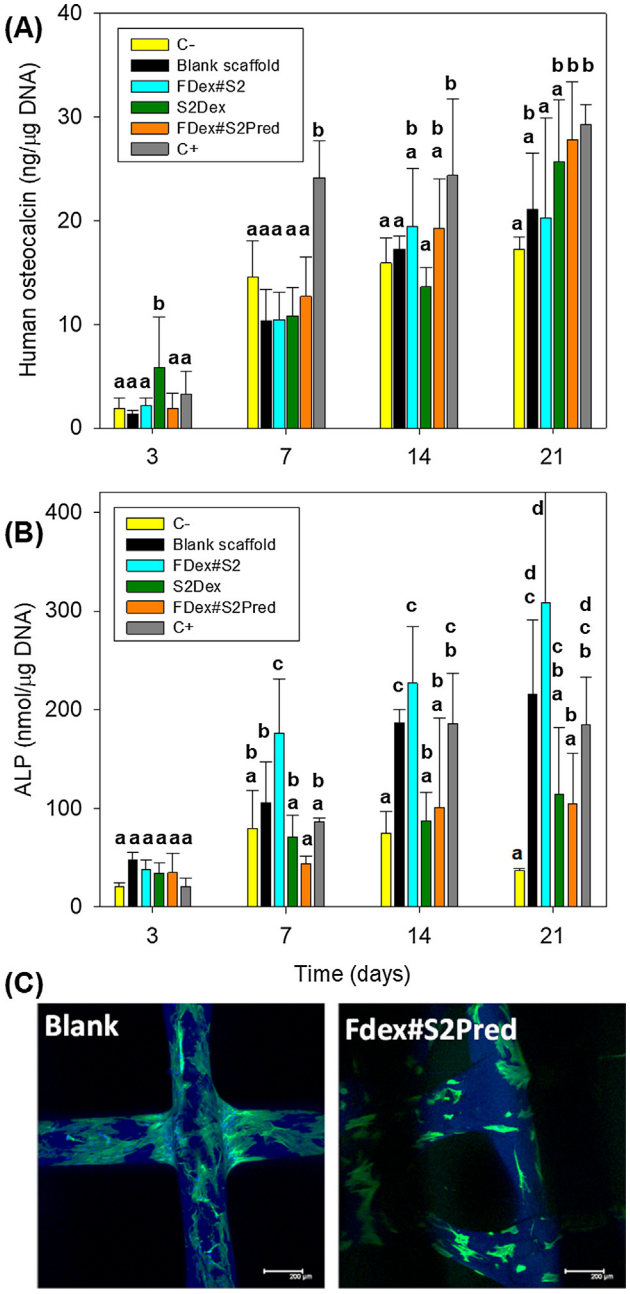

Fig. 7. Osteocalcin (A) and ALP activity (B) of hMSC incubated with the scaffolds. Negative control refers to cells growing in non-osteogenic medium (the same medium used for the scaffolds), while positive control refers to cells cultured in osteogenic medium. Equal letter denotes statistically homogenous groups (ANOVA and multiple range test $p < 0.05$; n = 3). (C) Confocal imaging of cell membrane (Alexa fluor 488 dye, green) and nuclei (DAPI, blue) of hMSCs cultured onto blank and dually loaded FDex#S2Pred scaffolds after 14 days incubation. Scale bar is 200 μm. (For interpretation of the references to colour in this figure legend, the reader is referred to the web version of this article.)

Osteocalcin is exclusively produced by osteoblasts, and thus it can be used as a preliminary biomarker for the effectiveness of the scaffolds themselves and of the loaded dexamethasone on the bone formation process. Only scaffolds containing dexamethasone at the surface (S2Dex) induced an increase in osteocalcin levels at day 3 (Fig. 7A). Growing in osteogenic medium caused an increase in osteocalcin at day 7, compared to the non-osteogenic medium, which was maintained for 21 days in good agreement with previous reports [53]. Interestingly, FDex#S2 showed maximum osteocalcin levels at day 14, while FDex#S2Pred reached the maximum at day 21, rendering levels similar to those recorded for the osteogenic medium (ANOVA; non-statistically significant differences). Both FDex#S2 and FDex#S2Pred have dexamethasone loaded inside the PLA strands and thus can sustainedly provide the cell culture medium with the osteogenic drug. The difference between these two scaffolds are related to the lower amount of dexamethasone released by FDex#S2Pred in the first incubation days, as expected from the release patterns showed in Fig. 5.

It should be noted that all scaffolds showed an excellent compatibility with hMSCs, rendering cell proliferation levels as high as or even above those of the negative control (Fig. S6 in Supporting Information file), which may be due to the fact that the scaffolds provided a 3D environment that favored cell growth compared to the 2D well surface. Indeed, after 14 days incubation the scaffold strands were covered by growing cells (Fig. 7C). Cells on blank scaffolds showed more extended cytoplasms compared to those growing on drug-loaded scaffolds, which may be related to the differentiation process.

Regarding ALP activity (Fig. 7B), cells cultured in non-osteogenic medium (negative control) and cells cultured in osteogenic medium (positive control) reached the maximum ALP activity at day 14 although showing remarkably different levels, also in good agreement with literature [53]. Then, the ALP levels decreased at day 21 in the case of the negative control but they were maintained in the positive control. Interestingly, the blank scaffold itself potentiated ALP activity at days 14 and 21 compared to the negative control (ANOVA and multiple range test $p < 0.05$). This finding is in agreement with previous papers that evidenced that the 3D architecture itself favors the differentiation of the hMSCs into osteoblast cells [54]. Relevantly, FDex#S2 induced earlier increase in ALP activity since day 7 (values statistically significant larger than positive control; ANOVA and multiple range test $p < 0.05$) and the activity continued growing until day 21, with values at day 14 similar to those recorded for the cells cultured in the osteogenic medium (positive control). At day 21, ALP values recorded for cells cultured in any of the scaffolds tested were higher than those recorded for the negative control

4. Conclusions

The step at which a drug is incorporated to a 3D printed scaffold notably determines the loading yield, the release rate and even the appearance and the morphology of the strands and their mechanical properties during biodegradation. During FDM printing, drugs loaded on the PLA filament may become solubilized in the melted PLA, which causes the drug to be molecularly dispersed in the printed strand matrix. At the doses tested such drug:PLA mixtures do not cause any detrimental change in the printability and the mechanical properties of the scaffolds, but ensure controlled release for several months under biorelevant conditions. Differently, loading of the drug after 3D printing leads to the coating of the strands with a layer of crystalline drug nanoparticles, which can exhibit burst release. Relevantly, post-manufacture loading of starting PLA filaments with one drug and of obtained printed scaffolds with a second drug allows tuning what drug would be loaded in higher amount and would be delivered first. All scaffolds exhibit excellent compatibility with fibroblast cells, macrophages and hMSC. Scaffolds loaded after printing with prednisolone (i.e., the drug on the surface) retain the anti-inflammatory activity of the drug, while scaffolds printed after dexamethasone loading of PLA filaments may induce faster and prolonged osteogenic differentiation.

Declaration of Competing Interest

The Authors declare that they have no conflicts of interest to disclose.

Acknowledgements

This work was funded by MINECO [SAF2017-83118-R], Agencia Estatal de Investigación (AEI) Spain, Xunta de Galicia [ED431C 2016/008; AEMAT ED431E 2018/08] and FEDER. The authors thank F. Alvarez-Rivera (University of Santiago de Compostela) and M.A. Grimaudo (University of Parma) for technical support during in vitro cell studies, and RIAIDT-USC for analytical facilities.

Appendix A. Supplementary material

Supplementary data to this article can be found online at https://doi.org/10.1016/j.ejpb.2019.05.018.

References

[1] A.V. Do, B. Khorsand, S.M. Geary, A.K. Salem, 3D printing of scaffolds for tissue regeneration applications, Adv. Healthc. Mater. 4 (2015) 1742–1762.
[2] N. Rodrigues, M. Benning, A.M. Ferreira, L. Dixon, K. Dalgarno, Manufacture and characterisation of porous PLA scaffolds, Procedia CIRP 49 (2016) 33–38.
[3] E. Babaie, S.B. Bhaduri, Fabrication aspects of porous biomaterials in orthopedic applications: a review, ACS Biomater. Sci. Eng. 4 (2018) 1–39.
[4] E.B. Petcu, R. Midha, E. McColl, A. Popa-Wagner, T.V. Chirila, P.D. Dalton, 3D printing strategies for peripheral nerve regeneration, Biofabrication 10 (2018) 032001.
[5] U. Ghosh, S. Ning, Y. Wang, Y.L. Kong, Addressing unmet clinical needs with 3D printing technologies, Adv. Healthc. Mater. 7 (2018) 1800417.
[6] J.E. Trachtenberg, P.M. Mountziaris, J.S. Miller, M. Wettergreen, F.K. Kasper, A.G. Mikos, Open-source three-dimensional printing of biodegradable polymer scaffolds for tissue engineering, J. Biomed. Mater. Res. A 102 (2014) 4326–4335.
[7] R. Akbarzadeh, A.M. Yousefi, Effects of processing parameters in thermally induced phase separation technique on porous architecture of scaffolds for bone tissue engineering, J. Biomed. Mater. Res. B Appl. Biomater. 102 (2014) 1304–1315.
[8] N. Thadavirul, P. Pavasant, P. Supaphol, Development of polycaprolactone porous scaffolds by combining solvent casting, particulate leaching, and polymer leaching techniques for bone tissue engineering, J. Biomed. Mater. Res. A 102 (2014) 3379–3392.
[9] J.R.C. Dizon, A.H. Espera, Q.Y. Chen, R.C. Advincula, Mechanical characterization of 3D-printed polymers, Additive Manufactur. 20 (2018) 44–67.
[10] L.G. Bracaglia, B.T. Smith, E. Watson, N. Arumugasaamy, A.G. Mikos, J.P. Fisher, 3D printing for the design and fabrication of polymer-based gradient scaffolds, Acta Biomater. 56 (2017) SI 3–13.
[11] C. Alvarez-Lorenzo, C.A. García-González, A. Concheiro, Cyclodextrins as versatile building blocks for regenerative medicine, J. Control Release 268 (2017) 269–281.
[12] D. Martinez-Marquez, A. Mirnajafizadeh, C.P. Carty, R.A. Stewart, Application of quality by design for 3D printed bone prostheses and scaffolds, PLoS ONE 13 (2018) e0195291.
[13] T. Serra, M.A. Mateos-Timoneda, J.A. Planell, M. Navarro, 3D printed PLA-based scaffolds, Organogenesis 9 (2013) 239–244.
[14] M.S. Lopes, A.L. Jardini, R.M. Filho, Poly(lactic acid) production for tissue engineering applications, Procedia Eng. 42 (Supplement C) (2012) 1402–1413.
[15] B.D. Ulery, L.S. Nair, C.T. Laurencin, Biomedical applications of biodegradable polymers, J. Polym. Sci. B Polym. Phys. 49 (2011) 832–864.
[16] J. Goole, K. Amighi, 3D printing in pharmaceutics: A new tool for designing customized drug delivery systems, Int. J. Pharm. 499 (2016) 376–394.
[17] J. An, J.E.M. Teoh, R. Suntornnond, C.K. Chua, Design and 3D printing of scaffolds and tissues, Engineering 1 (2015) 261–268.
[18] E. Ceretti, P. Ginestra, P. Neto, A. Fiorentino, J. Da Silva, Multi-layered scaffolds production via Fused Deposition Modeling (FDM) using an open source 3D printer: process parameters optimization for dimensional accuracy and design reproducibility, Procedia CIRP 65 (2017) 13–18.
[19] W. Kempin, C. Franz, L.C. Koster, F. Schneider, M. Bogdahn, W. Weitschies, A. Seidlitz, Assessment of different polymers and drug loads for fused deposition modeling of drug loaded implants, Eur. J. Pharm. Biopharm. 115 (2017) 84–93.
[20] J. Boetker, J.J. Water, J. Aho, L. Arnfast, A. Bohr, J. Rantanen, Modifying release characteristics from 3D printed drug-eluting products, Eur. J. Pharm. Sci. 90 (2016) 47–52.
[21] L.E. Visscher, H.P. Dang, M.A. Knackstedt, D.W. Hutmacher, P.A. Tran, 3D printed polycaprolactone scaffolds with dual macro-microporosity for applications in local delivery of antibiotics, Mat. Sci. Eng. C 87 (2018) 78–89.
[22] P.F. Costa, A.M. Puga, L. Díaz-Gomez, A. Concheiro, D.H. Busch, C. Alvarez-Lorenzo, Additive manufacturing of scaffolds with dexamethasone controlled release for enhanced bone regeneration, Int. J. Pharm. 496 (2015) 541–550.
[23] C.J. Bloomquist, M.B. Mecham, M.D. Paradzinsky, R. Janusziewicz, S.B. Warner, J.C. Luft, S.J. Mecham, A.Z. Wang, J.M. DeSimone, Controlling release from 3D printed medical devices using CLIP and drug-loaded liquid resins, J. Control. Release 278 (2018) 9–23.
[24] T. Maver, D.M. Smrke, M. Kurečič, L. Gradišnik, U. Maver, K.S. Kleinschek, Combining 3D printing and electrospinning for preparation of pain relieving wound-dressing materials, J. Sol-Gel Sci. Tech. 88 (2018) 33–48.
[25] J. Holländer, N. Genina, H. Jukarainen, M. Khajeheian, A. Rosling, E. Mäkilä, N. Sandler, Three-dimensional printed PCL-based implantable prototypes of medical devices for controlled drug delivery, J. Pharm. Sci. 105 (2016) 2665–2676.
[26] P.M. Mountziaris, P.P. Spicer, F.K. Kasper, A.G. Mikos, Harnessing and modulating inflammation in strategies for bone regeneration, Tissue Eng. Part B Rev. 17 (2011) 393–402.
[27] M. Kokavec, M. Fristakova, P. Polan, G.M. Bialik, Surgical options for the treatment of simple bone cyst in children and adolescents, IMAJ 12 (2010) 87–90.
[28] X. Shi, L. Ren, M. Tian, J. Yu, W. Huang, C. Du, D.A. Wang, Y. Wang, In vivo and in vitro osteogenesis of stem cells induced by controlled release of drugs from microspherical scaffolds, J. Mater. Chem. 20 (2010) 9140–9148.
[29] A. Lima, A.M. Puga, J. Mano, A. Concheiro, C. Alvarez-Lorenzo, Free and copolymerized γ-cyclodextrins regulate the performance of dexamethasone-loaded dextran microspheres for bone regeneration, J. Mater. Chem. B 2 (2014) 4943–4956.
[30] A. Goyanes, A.B. Buanz, A.W. Basit, S. Gaisford, Fused-filament 3D printing (3DP) for fabrication of tablets, Int. J. Pharm. 476 (2014) 88–92.
[31] A. Goyanes, A.B. Buanz, G.B. Hatton, S. Gaisford, A.W. Basit, 3D printing of modified-release aminosalicylate (4-ASA and 5-ASA) tablets, Eur. J. Pharm. Biopharm. 89 (2015) 157–162.
[32] J. Skowyra, K. Pietrzak, M.A. Alhnan, Fabrication of extended-release patient-tailored prednisolone tablets via fused deposition modelling (FDM) 3D printing, Eur. J. Pharm. Sci. 68 (2015) 11–17.
[33] R.C.R. Beck, P.S. Chaves, A. Goyanes, B. Vukosavljevic, A. Buanz, M. Windbergs, A.W. Basit, S. Gaisford, 3D printed tablets loaded with polymeric nanocapsules: An innovative approach to produce customized drug delivery systems, Int. J. Pharm. 528 (2017) 268–279.
[34] H. Hashem, T. Jira, Chromatographic applications on monolithic columns: determination of triamcinolone, prednisolone and dexamethasone in pharmaceutical tablet formulations using a solid phase extraction and a monolithic column, Chromatographia 61 (2005) 133–136.
[35] E.W. Fischer, J.S. Hans, G. Wegner, Investigation of the structure of solution grown crystals of lactide copolymers by means of chemical reactions, Colloid Polym. Sci. 251 (1973) 980–990.
[36] J. Wang, H. Chen, Z. Chen, Y. Chen, D. Guo, M. Ni, S. Liu, C. Peng, In-situ formation of silver nanoparticles on poly(lactic acid) film by γ-radiation induced grafting of N-vinyl pyrrolidone, Mater. Sci. Eng. C 63 (2016) 142–149.
[37] R.P. Konstance, Axial-compression properties of calcium caseinate gels, J. Dairy Sci. 76 (1993) 3317–3326.
[38] R. Ipsen, Uniaxial compression of gels made from protein and k-carragenan, J. Texture Stud. 28 (1997) 405–419.
[39] E. Llorens, L.J. del Valle, J. Puiggalí, Multifunctional ternary drug-loaded electrospun scaffolds, J. Appl. Polym. Sci. 133 (2016) 42751.
[40] P. Diaz-Rodriguez, M. Landin, Controlled release of indomethacin from alginate-poloxamer-silicon carbide composites decrease in-vitro inflammation, Int. J. Pharm. 480 (2015) 92–100.
[41] S.H. Yalkowsky, R.M. Dannenfelser, Aquasol database of aqueous solubility, College of Pharmacy, University of Arizona, 1992.
[42] D.X. Li, G. Guo, R.R. Fan, J. Liang, X. Deng, F. Luo, Z.Y. Qian, PLA/F68/Dexamethasone implants prepared by hot-melt extrusion for controlled release of anti-inflammatory drug to implantable medical devices: I. Preparation, characterization and hydrolytic degradation study, Int. J. Pharm. 441 (2013) 365–372.
[43] S. Sato, D. Gondo, T. Wada, S. Kanehashi, K. Nagai, Effects of various liquid organic solvents on solvent-induced crystallization of amorphous poly (lactic acid) film, J. Appl. Polym. Sci. 129 (2013) 1607–1617.
[44] L. Goimil, P. Jaeger, I. Ardao, J.L. Gómez-Amoza, A. Concheiro, C. Alvarez-Lorenzo, C.A. García-González, Preparation and stability of dexamethasone-loaded polymeric scaffolds for bone regeneration processed by compressed CO_2 foaming, J. CO2 Utilization 24 (2018) 89–98.
[45] B.M. Frey, F.J. Frey, Clinical pharmacokinetics of prednisone and prednisolone, Clin. Pharmacokinet. 19 (1990) 126–146.
[46] M. Savioli Lopes, A.L. Jardini, Filho R. Maciel, Poly(lactic acid) production for tissue engineering applications, Procedia Eng. 42 (2012) 1402–1413.
[47] S.M. Alshahrani, J.T. Morott, A.S. Alshetaili, R.V. Tiwari, S. Majumdar, M.A. Repka, Influence of degassing on hot-melt extrusion process, Eur. J. Pharm. Sci. 80 (2015) 43–52.
[48] M. Hesami, A. Jalali-Arani, Cold crystallization behavior of poly(lactic acid) in its blend with acrylic rubber; the effect of acrylic rubber content, Polym. Int. 66 (2017) 1564–1571.
[49] K.A. Athanasiou, C. Zhu, D.R. Lanctot, C.M. Agrawal, X. Wang, Fundamentals of biomechanics in tissue engineering of bone, Tissue Eng. 6 (2000) 361–381.
[50] J. Shen, D.J. Burgess, Accelerated in-vitro release testing methods for extended-release parenteral dosage forms, J. Pharm. Pharmacol. 64 (2012) 986–996.
[51] S.A.M. Ali, P.J. Doherty, D.F. Williams, Molecular biointeractions of biomedical polymers with extracellular exudates and inflammatory cells and their effects on biocompatibility, in vivo, Biomaterials 15 (1994) 779–785.
[52] J. Henkel, M.A. Woodruff, D.R. Epari, R. Steck, V. Glatt, I.C. Dickinson, P.F.M. Choong, M.A. Schuetz, D.W. Hutmacher, Bone regeneration based on tissue engineering conceptions – A 21st century perspective, Bone Res. 3 (2013) 216–248.
[53] P. Arpornmaeklong, S.E. Brown, Z. Wang, P.H. Krebsbach, Phenotypic characterization, osteoblastic differentiation, and bone regeneration capacity of human embryonic stem cell–derived mesenchymal stem cells, Stem Cells Development 18 (2009) 955–968.
[54] M. Persson, P.P. Lehenkari, L. Berglin, S. Turunen, M.A.J. Finnilä, J. Risteli, M. Skrifvars, J. Tuukkanen, Osteogenic differentiation of human mesenchymal stem cells in a 3D woven scaffold, Sci. Rep. 8 (2018) 10457.